

Department of Physics and Astronomy
Heidelberg University

Bachelor Thesis in Physics
submitted by

Romain Chazotte

born in Cologne (Germany)

2022

Recoil correction to the energy levels of heavy muonic atoms

This Bachelor Thesis has been carried out by Romain Chazotte at the
Max Planck Institute for Nuclear Physics in Heidelberg
under the supervision of
Dr. Natalia S. Oreshkina

Abstract

In this work, the relativistic recoil correction to the energies of heavy muonic atoms has been considered, based on the formalism suggested by Borie and Rinker.

Muonic atoms are atoms, which have a bound muon instead of an electron. The lifetime of a muon is long enough so it can be considered stable on the atomic scale. Additionally, an atom with a single bound muon can be considered as a hydrogen-like system. As muons are about 200 times heavier than electrons, they orbit the nucleus 200 times closer. This leads to a larger contribution of all kinds of nuclear effects to the energy levels of the muon.

We calculated the recoil effect for the shell, sphere and Fermi nuclear models and studied model and nuclear parameters dependence. Additionally, we compared the results with previous studies. Going forward, the results can be used for high-precision theoretical predictions of the spectra of heavy muonic atoms, and in further comparison with experimental data, aiming at the extraction of nuclear properties and parameters. In the future, a more rigorous quantum electrodynamics formalism can be applied to enhance the accuracy of the relativistic recoil effect.

Zusammenfassung

In dieser Arbeit wurde die relativistische Rückstoßkorrektur auf die Energieniveaus schwerer Myonatome betrachtet, basierend auf dem von Borie und Rinker vorgeschlagenem Formalismus.

Myonische Atome sind Atome, die ein gebundenes Myon anstelle eines Elektrons haben. Die Lebensdauer eines Myons ist lang genug, dass es auf atomarer Skala als stabil angesehen werden. Außerdem kann ein Atom mit einem einzelnen gebundenen Myon als wasserstoffähnliches System betrachtet werden. Da Myonen etwa 200-mal schwerer sind als Elektronen, umkreisen sie den Kern 200-mal näher. Dies führt zu einem größeren Beitrag aller Arten von nuklearen Effekten zu den Energieniveaus des Myons.

Wir haben den Rückstoßeffect für das Schalen-, Kugel- und Fermi-Kernmodell berechnet und die Abhängigkeit von Modell- und Kernparametern untersucht. Darüber hinaus haben wir die Ergebnisse mit früheren Studien verglichen. In Zukunft können die Ergebnisse für hochpräzise theoretische Vorhersagen der Spektren von schweren Myonatomen und im weiteren Vergleich mit experimentellen Daten verwendet werden, die auf die Extraktion von Kerneigenschaften und Parametern abzielen.

Contents

1	Introduction	2
2	Energy correction	4
2.1	Necessary formulas	4
2.2	Point-like-nucleus	5
2.3	Q_4 calculation	5
2.4	Shell nuclear model	6
2.5	Sphere nuclear model	6
2.6	Fermi nuclear model	7
3	Results	8
3.1	Recoil correction in comparison to previous results	13
3.2	Recoil correction for a few selected atoms	14
3.3	Nuclear size sensitivity	16
3.4	Numerical accuracy	19
3.5	Different uncertainties in comparison	20
3.6	Different models	23
4	Model dependence and outlook	24

1 Introduction

The inner structure of atomic nuclei is of great interest to fundamental physics. One way to further improve the understanding of the fine structure is to research muonic atoms. These are atoms, which have accumulated a muon, replacing an electron. The lifetime of a muon is long enough as to be considered bound on a nuclear time-scale. By comparing experimental results to our theoretical predictions, we can learn more about the atomic structure.

As muons have approximately 200 times the mass of an electron the muons Bohr radius is smaller by the same factor and the muon can be considered to be in a hydrogen-like atom [1]. Therefore, different energy corrections can be recorded more clearly as two-particle interactions do not have a significant impact. Furthermore, as the nucleus is far bigger in relative units considered by the muon, nuclear effects play a far more significant role. In fact, as seen in Figure 1, a big part of the muonic wave function even is inside of the nucleus for heavy nuclei.

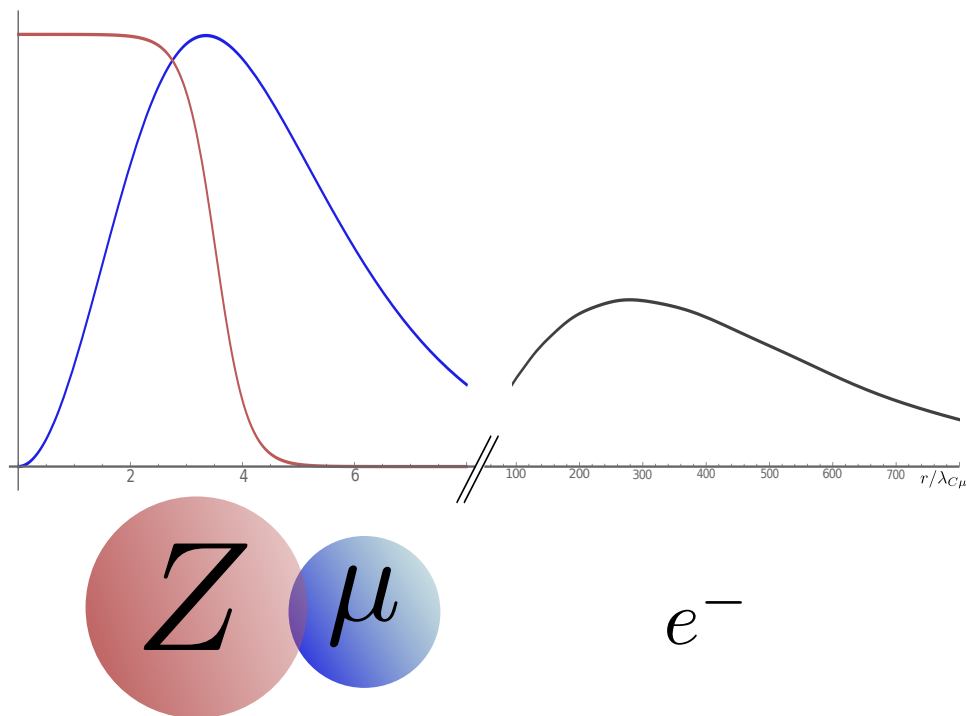


Figure 1: Charge distribution of the nucleus (red), the $1s_{1/2}$ wave-function of the muon (blue), and electron (gray, enhanced by a factor of 50) for Hydrogen-like Uranium. The figure is taken from [1].

The aim of this work is to calculate one of the nuclear effects, namely the recoil effect. Nuclear recoil corrections for muonic atoms can be calculated by using the reduced mass μ , given by $\frac{mM}{m+M}$, where m is the mass of the muon and M the mass of the nucleus. This can be calculated by expanding in αZ , $\alpha \approx \frac{1}{137}$ being the fine structure constant and Z being the nuclear charge. For nuclei with higher Z an expansion in αZ is not viable anymore, as αZ comes closer to 1, therefore another method has to be used. For that the approach of [2, 3] to expand in m/M is used. This approach is completely rigorous, in contrast to the classical Bethe-Salpeter solution [2]. The energy correction is then calculated following the procedure described in [1, 4]. The calculation using the B-splines method as by [5, 6] is done for different nuclear models and can be executed for any isotope.

On the scale of muonic atoms, the relativistic nuclear recoil effect has a great impact on the energy levels. In fact, as can be seen in Table 1 for the ground and some excited states of ^{248}Cm , the finite size recoil contribution is much larger than the point-like model contribution. Thus, it is very interesting to calculate this term.

state	$\Delta E_{nk,sphere}^{(rec,fin)}$	$\Delta E_{nk,point}^{(rec)}$
$1s_{1/2}$	352	62
$2s_{1/2}$	46	63
$2p_{1/2}$	88	74
$2p_{3/2}$	82	61
$3s_{1/2}$	12	27
$3p_{1/2}$	18	28
$3p_{3/2}$	17	24
$3d_{3/2}$	19	7
$3d_{5/2}$	18	5

Table 1: The finite size energy correction and leading order point like approximation energy correction both listed for ^{248}Cm . Energies given in eV

The nuclear radii needed for the calculations were taken from [7], the nuclear masses from [8].

In our work we considered three different nuclear models, the shell, sphere and Fermi model. The shell model gives relatively easy calculations and is thus useful for low precision finite size nuclear calculations.

The sphere model is a more realistic yet more complicated model.

In the Fermi model the charge distribution follows a Fermi distribution. This model more precisely represents the nuclear structure as it also models a “skin”, where the distribution falls off rapidly yet continuously.

2 Energy correction

In this work relativistic muonic units are used with $\hbar = c = m_\mu = 1$, m_μ being the muonic mass, c the speed of light and \hbar the reduced Planck constant.

We calculate the relativistic recoil energy correction for muonic atoms, given by [1]:

$$\Delta E_{nk}^{(rec,rel)} = -\frac{(E_{nk}^{(fm)})^2}{2M_N} + \frac{1}{2M_N} \langle h(r) + 2E_{nk}^{(fm)} P_1(r) \rangle. \quad (1)$$

Here, M_N is the nuclear mass, $E_{nk}^{(fm)}$ the binding energy given by solving the Dirac equation [1]. $P_1(r)$ and $h(r)$ are defined in chapter 2.1. To convert this from relativistic units to eV, one writes:

$$\Delta E_{nk}^{(rec,rel)} [eV] = \Delta E_{nk}^{(rec,rel)} \frac{m_\mu}{M_N} m_\mu c^2. \quad (2)$$

2.1 Necessary formulas

For the calculation of the energy correction, we need the following equations given as Eqs. (109) and (111) of [4]. $V(r)$ denotes the nuclear potential.

$$P_1(r) = -rV'(r) - V(r), \quad (3)$$

$$Q_2(r) = r^2V'(r), \quad (4)$$

$$Q_4(r) = r^4V'(r) - 2r^3V(r) + 6 \int_0^r x^2V(x)dx. \quad (5)$$

For simplicity, this can be divided into three parts:

$$Q_{41}(r) = r^4V'(r),$$

$$Q_{42}(r) = -2r^3V(r),$$

$$Q_{43}(r) = 6 \int_0^r x^2V(x)dx,$$

with Q_4 then being:

$$Q_4(r) = \sum Q_{4i}(r).$$

Now $h(r)$ is made up of these:

$$h(r) = -\left(P_1(r)^2 + \frac{4P_1(r)Q_2(r)}{3r} + \frac{Q_2(r)Q_4(r)}{3r^4} \right). \quad (6)$$

2.2 Point-like-nucleus

The recoil correction to the energy in the point-like-nucleus approximation itself is not interesting to us, as it is the exact model that ignores all finite size nuclear effects. This model is useful for calculations of regular atoms. We still calculate formulas 3, 4, 5 and 6, as both the sphere- and shell-like nuclear model give the same potential as the point-like nuclear model outside of the nucleus.

For the point-like model the nuclear potential is simply given by:

$$V(r) = -\alpha Z/r. \quad (7)$$

This now gives:

$$\begin{aligned} P_1(r) &= \alpha Z/r - \alpha Z/r = 0, \\ Q_2(r) &= \alpha Z, \\ Q_{41}(r) &= \alpha Z r^2, \\ Q_{42}(r) &= 2\alpha Z r^2, \\ Q_{43}(r) &= -3\alpha Z r^2, \\ Q_4(r) &= \sum Q_{4i}(r) = 0, \\ h(r) &= 0. \end{aligned} \quad (8)$$

2.3 Q_4 calculation

Both the shell nuclear model and the sphere nuclear model have the same potential as the point-like nuclear model for $r > rm_{nucl}$, rm_{nucl} being the nuclear root mean square radius. For most of the functions above, this gives a trivial result. However, for Q_{43} it is more complicated as there is an integral involved. Here, for $r' > rm_{nucl}$ we have:

$$\begin{aligned} Q_{43}(r') &= 6 \int_0^{r'} x^2 V(x) dx = 6 \int_0^{rm_{nucl}} x^2 V(x) dx + 6 \int_{rm_{nucl}}^{r'} x^2 V(x) dx \\ &= 6 \int_0^{rm_{nucl}} x^2 V(x) dx + 3\alpha Z rm_{nucl}^2 + Q_{43,point}(r'). \end{aligned} \quad (10)$$

Therefore we get:

$$\begin{aligned} Q_4(r) &= \sum Q_{4i}(r) = \sum Q_{4i,point}(r) + 6 \int_0^{rm_{nucl}} x^2 V(x) dx + 3\alpha Z rm_{nucl}^2 \\ &= Q_{43}(rm_{nucl}) + 3\alpha Z rm_{nucl}^2. \end{aligned} \quad (11)$$

2.4 Shell nuclear model

For $r < rm_{nucl}$ we get:

$$V(r) = -\alpha Z/rm_{nucl}, \quad (12)$$

$$P_1(r) = \alpha Z/rm_{nucl}, \quad (13)$$

$$Q_2(r) = 0,$$

$$Q_{41}(r) = 0,$$

$$Q_{42}(r) = \alpha Z 2r^3/rm_{nucl},$$

$$Q_{43}(r) = -2\alpha Z r^3/rm_{nucl},$$

$$Q_4(r) = \sum Q_{4i}(r) = 0,$$

$$h(r) = -(\alpha Z/rm_{nucl})^2 + 0 + 0 = -(\alpha Z/rm_{nucl})^2. \quad (14)$$

For $r > rm_{nucl}$, the potential is equal to that of a point-like model, therefore:

$$P_1(r) = 0,$$

$$Q_2(r) = \alpha Z.$$

Q_4 is defined by Eq.(11) and therefore gives for the shell model of the nucleus:

$$Q_4(r) = -2\alpha Z rm_{nucl}^2 + 3\alpha Z rm_{nucl}^2 = \alpha Z rm_{nucl}^2, \quad (15)$$

$$h(r) = -\frac{Q_2(r)Q_4(r)}{3r^4} = -\frac{(\alpha Z rm_{nucl})^2}{3r^4}. \quad (16)$$

2.5 Sphere nuclear model

for $r < rm_{nucl}$ we get:

$$V(r) = -\alpha Z(3/2 - 1/2(r/rm_{nucl})^2)/rm_{nucl}, \quad (17)$$

$$P_1(r) = -\alpha Z r^2/rm_{nucl}^3 + \alpha Z(3/2 - 0.5(r/rm_{nucl})^2)/rm_{nucl}, \quad (18)$$

$$Q_2(r) = \alpha Z(r/rm_{nucl})^3,$$

$$Q_{41}(r) = \alpha Z r^5/rm_{nucl}^3,$$

$$Q_{42}(r) = 3r^3\alpha Z/rm_{nucl} - \alpha Z r^5/rm_{nucl}^3,$$

$$Q_{43}(r) = -3\alpha Z r^3/rm_{nucl} + (3/5)\alpha Z r^5/rm_{nucl}^3,$$

$$Q_4(r) = \alpha Z r^5 / r m_{nucl}^3 + 3r^3 \alpha Z / r m_{nucl} - \alpha Z r^5 / r m_{nucl}^3 - 3\alpha Z r^3 / r m_{nucl} + (3/5)\alpha Z r^5 / r m_{nucl}^3$$

$$= (3/5)\alpha Z r^5 / r m_{nucl}^3,$$

$$h(r) = -P_1(r)^2 - \frac{4P_1(r)Q_2(r)}{3r} - \frac{Q_2(r)Q_4(r)}{3r^4}. \quad (19)$$

For $r > r m_{nucl}$, the potential is equal to that of a point-like model, therefore:

$$P_1(r) = 0,$$

$$Q_2(r) = \alpha Z.$$

Q_4 is defined by Eq.(11) and therefore gives for the sphere model of the nucleus:

$$Q_4(r) = -3\alpha Z r m_{nucl}^2 + (3/5)\alpha Z r m_{nucl}^2 + 3\alpha Z r m_{nucl}^2 = (3/5)\alpha Z r m_{nucl}^2, \quad (20)$$

$$h(r) = -Q_2(r)Q_4(r)/(3r^4) = -\frac{(\alpha Z r m_{nucl})^2}{5r^4}. \quad (21)$$

2.6 Fermi nuclear model

For the Fermi nuclear model the nuclear charge distribution is given by a Fermi distribution:

$$\rho(r) = \frac{\rho_0}{1 + e^{(r-c)/a}}, \quad (22)$$

c, a and ρ_0 being constants. As analytical calculations for the Fermi model are very complicated, we use Eq.(3.2) from [9] and solve it by numerical methods. The uncertainty of this procedure can be estimated by comparing the semi-analytical values of the other models with the numerical ones, as the numerical formalism could in principle be applied to all nuclear models.

3 Results

Here we present the results of the calculation for a few selected isotopes in the different models.

We calculate both the semi-analytical values and the numerical ones. For the semi-analytical values the Eqs. (3, 4, 5, 6) have been calculated analytically and the averaging in Eq. (1) is done numerically. The numerical values are calculated by having Eqs. (1, 3, 4, 5, 6) calculated numerically.

The amount of splines used for the calculations in this work is 70, if not otherwise indicated. 70 was chosen as more splines did not have a considerable impact on the results, yet would have taken more computing time.

As by using a higher number of splines the semi-analytical value did not change significantly while the numerical value was slowly growing towards the semi-analytical one, the semi-analytical value was used where possible.

The uncertainties indicated in brackets are estimated by calculating the difference in the semi-analytical value and the numerical one. The semi-analytical value was found to be bigger for every value. This uncertainty seems like a good approximation, as both models use numerical methods. However, increasing the number of splines from 70 to 90 changed the semi-analytical values in only about the seventh digit, while increasing the numerical ones in the fifth. Thus, these uncertainties might be assumed higher than they actually are. Furthermore, it could be that the error isn't solvable by adding a reasonable amount of splines so this uncertainty is assumed reasonable. The results for ^{89}Zr and ^{248}Cm are plotted in Figure 2, the $1s_{1/2}$ states of all considered atoms in Figure 3, the $2p_{1/2}$ states in Figure 4, and the $3d_{3/2}$ states in Figure 5.

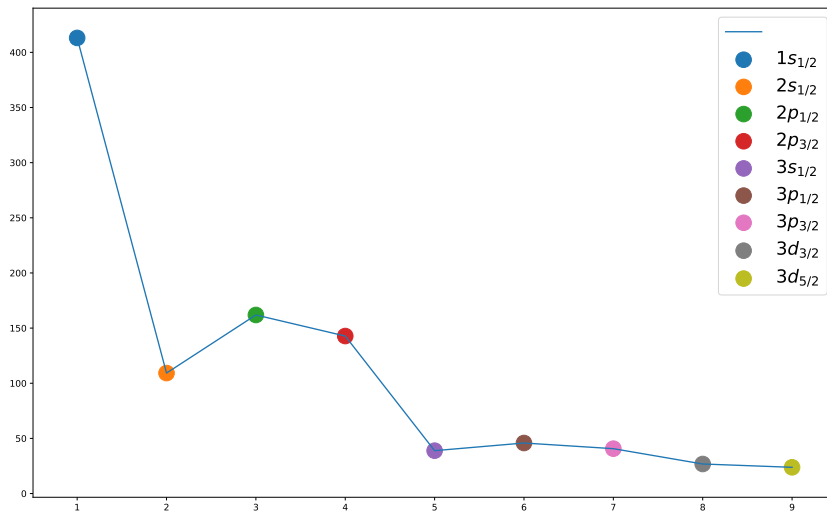
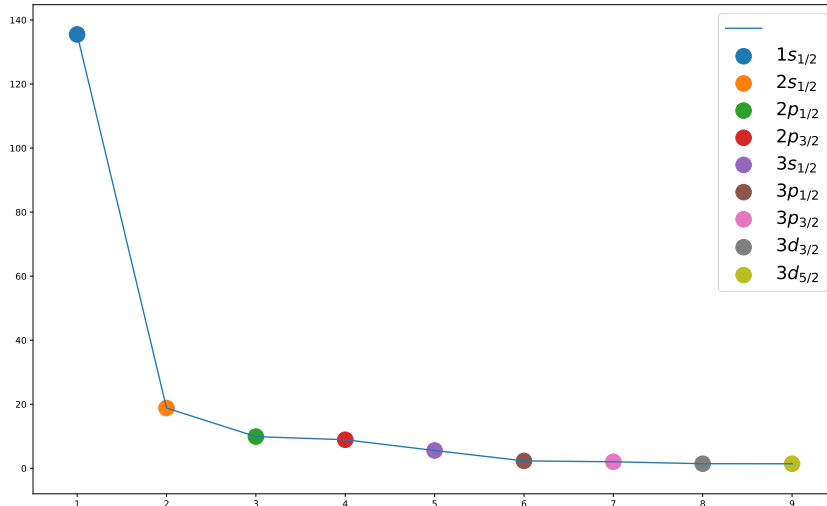


Figure 2: The energy levels of the different states first for ^{89}Zr , given by Table 2, and second for ^{248}Cm , given by Table 9. One can see a relative increase of the p states. Energy given in eV.

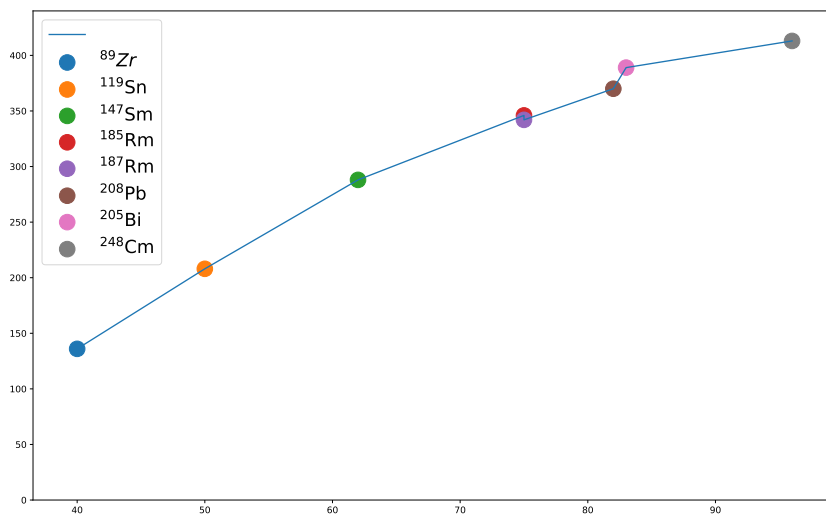


Figure 3: The $1s_{1/2}$ state energies for all considered isotopes with Z on the x-axis. The energy seems to increase with the number of protons Z , yet get smaller with the number of neutrons. Energy given in eV.

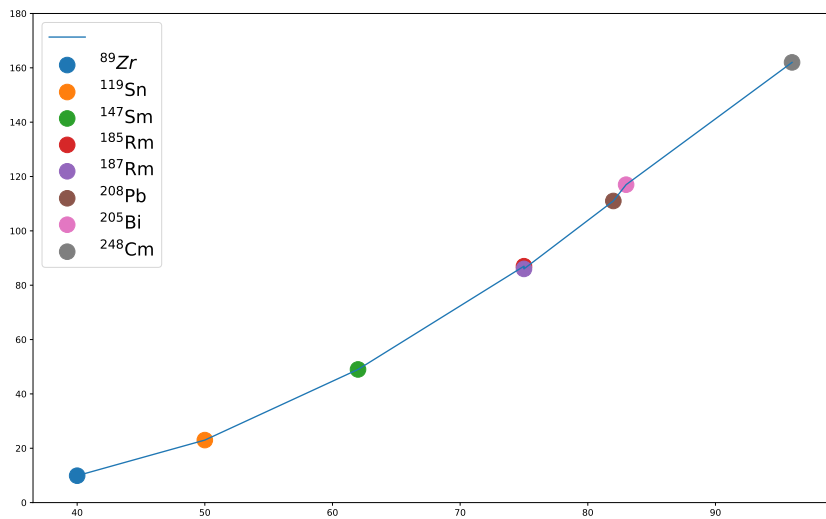


Figure 4: The $2p_{1/2}$ state energies for all considered isotopes, with Z on the x-axis. The energy seems to show exponential features with the number of protons Z , especially considering that the scale starts at $Z = 37$ and $E = 0$. Neutrons seem to have a smaller impact then for the $1s$ state. Energy given in eV.

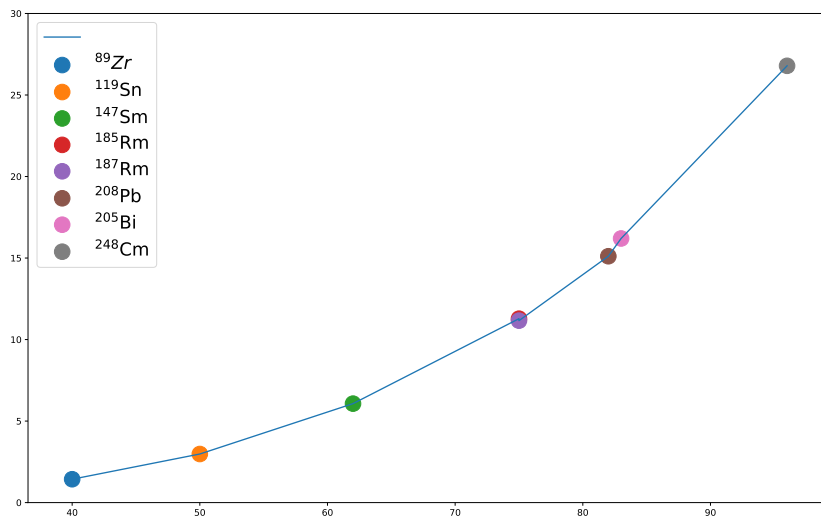


Figure 5: The $3d_{3/2}$ state energies for all considered isotopes, with Z on the x-axis. The energy seems to show even more exponential features than the $2p_{1/2}$ state energies, again with the scale starting at $Z = 37$ and $E = 0$. Neutrons seem to have a smaller impact than for the $1s$ state. Energy given in eV.

3.1 Recoil correction in comparison to previous results

We calculated the recoil correction for $^{89}_{40}\text{Zr}$ (Table 2), $^{147}_{62}\text{Sm}$ (Table 3) and $^{205}_{83}\text{Bi}$ (Table 4) and compared these values with the ones found in [1]. Their calculations are done with the Fermi model and while their values are not very precise, the uncertainty oftentimes being as large as the value itself, the values are very useful in order to check whether any bigger mistakes have been made. This does not seem to be the case, as all calculated values are within a reasonable range of their counterpart.

state	$\Delta E_{nk,sphere}^{(rec,rel)}$	$\Delta E_{nk,shell}^{(rec,rel)}$	$\Delta E_{nk,fermi}^{(rec,rel)}$	$\Delta E_{nk,michel}^{(rec,rel)}$
$1s_{1/2}$	135.5 (3)	134.1 (4)	135.2	150(150)
$2s_{1/2}$	18.82(5)	18.70 (5)	18.77	20(20)
$2p_{1/2}$	9.90 (6)	9.91 (7)	9.83	10(10)
$2p_{3/2}$	8.92 (6)	8.93 (6)	8.85	10(10)
$3s_{1/2}$	5.558 (16)	5.534 (17)	5.540	10(10)
$3p_{1/2}$	2.316 (19)	2.32 (2)	2.295	0
$3p_{3/2}$	2.036 (18)	2.037 (19)	2.017	0
$3d_{3/2}$	1.433 (11)	1.433 (12)	1.421	0
$3d_{5/2}$	1.415 (11)	1.415 (12)	1.403	0

Table 2: Recoil correction for a few first states of muonic ^{89}Zr . Energy given in eV.

state	$\Delta E_{nk,sphere}^{(rec,rel)}$	$\Delta E_{nk,shell}^{(rec,rel)}$	$\Delta E_{nk,fermi}^{(rec,rel)}$	$\Delta E_{nk,michel}^{(rec,rel)}$
$1s_{1/2}$	288.4 (5)	280.4 (5)	287.8	290(70)
$2s_{1/2}$	52.48 (10)	51.32 (10)	52.38	50(50)
$2p_{1/2}$	48.72 (19)	49.12 (2)	48.52	50(50)
$2p_{3/2}$	41.78 (19)	42.21 (19)	41.59	40(40)
$3s_{1/2}$	16.72 (3)	16.43 (3)	16.69	20(20)
$3p_{1/2}$	12.57 (5)	12.65 (6)	12.51	10(10)
$3p_{3/2}$	10.64 (5)	10.74 (6)	10.58	10(10)
$3d_{3/2}$	6.07 (4)	6.06 (4)	6.02	10(10)
$3d_{5/2}$	5.82 (4)	5.82 (4)	5.78	10(10)

Table 3: Recoil correction for a few first states of muonic ^{147}Sm . Energy given in eV.

state	$\Delta E_{nk,sphere}^{(rec,rel)}$	$\Delta E_{nk,shell}^{(rec,rel)}$	$\Delta E_{nk,fermi}^{(rec,rel)}$	$\Delta E_{nk,michel}^{(rec,rel)}$
$1s_{1/2}$	389.1 (6)	371.8 (5)	388.5	390(40)
$2s_{1/2}$	89.27 (14)	85.60 (13)	89.13	90(30)
$2p_{1/2}$	116.5 (3)	118.1 (3)	116.2	120(30)
$2p_{3/2}$	100.7 (3)	102.8 (3)	100.4	10(10)
$3s_{1/2}$	30.45 (5)	29.42 (5)	30.40	30(30)
$3p_{1/2}$	31.79 (9)	32.07 (9)	31.70	30(30)
$3p_{3/2}$	27.54 (9)	28.03 (9)	27.45	30(30)
$3d_{3/2}$	16.20 (8)	16.22 (9)	16.11	20(20)
$3d_{5/2}$	14.84 (8)	14.84 (8)	14.76	20(20)

Table 4: Recoil correction for a few first states of muonic ^{205}Bi . Energy given in eV.

3.2 Recoil correction for a few selected atoms

Additionally, we calculated the nuclear recoil effect energy correction for a few more atoms, $^{208}_{82}\text{Pb}$ (Table 5), $^{119}_{50}\text{Sn}$ (Table 6), $^{185}_{75}\text{Re}$ (Table 7), $^{187}_{75}\text{Re}$ (Table 8) and $^{248}_{96}\text{Cm}$ (Table 9).

state	$\Delta E_{nk,sphere}^{(rec,rel)}$	$\Delta E_{nk,shell}^{(rec,rel)}$	$\Delta E_{nk,fermi}^{(rec,rel)}$
$1s_{1/2}$	372.0 (5)	355.7 (5)	371.4
$2s_{1/2}$	84.64 (13)	81.23 (12)	84.51
$2p_{1/2}$	109.5 (3)	110.9 (3)	109.1
$2p_{3/2}$	94.6 (3)	96.5 (3)	94.3
$3s_{1/2}$	28.80 (5)	27.84 (4)	28.75
$3p_{1/2}$	29.80 (9)	30.06 (9)	29.71
$3p_{3/2}$	25.80 (8)	26.26 (9)	25.72
$3d_{3/2}$	15.11 (8)	15.13 (8)	15.03
$3d_{5/2}$	13.87 (7)	13.87 (8)	13.80

Table 5: Recoil correction for a few first states of muonic ^{208}Pb . Energy given in eV.

state	$\Delta E_{nk,sphere}^{(rec,rel)}$	$\Delta E_{nk,shell}^{(rec,rel)}$	$\Delta E_{nk,fermi}^{(rec,rel)}$
$1s_{1/2}$	207.8 (4)	204.0 (4)	207.3
$2s_{1/2}$	32.78 (8)	32.36 (8)	32.71
$2p_{1/2}$	22.82 (12)	22.92 (12)	22.70
$2p_{3/2}$	19.93 (11)	20.02 (11)	19.81
$3s_{1/2}$	10.03 (2)	9.93 (2)	10.01
$3p_{1/2}$	5.63 (3)	5.65 (4)	5.60
$3p_{3/2}$	4.81 (3)	4.83 (3)	4.78
$3d_{3/2}$	2.98 (2)	2.98 (2)	2.96
$3d_{5/2}$	2.92 (2)	2.92 (2)	2.90

Table 6: Recoil correction for a few first states of muonic ^{119}Sn . Energy given in eV.

state	$\Delta E_{nk,sphere}^{(rec,rel)}$	$\Delta E_{nk,shell}^{(rec,rel)}$	$\Delta E_{nk,fermi}^{(rec,rel)}$
$1s_{1/2}$	346.4 (5)	333.1 (5)	345.8
$2s_{1/2}$	73.26 (12)	70.77 (11)	73.14
$2p_{1/2}$	86.5 (3)	87.5 (3)	86.2
$2p_{3/2}$	74.3 (2)	75.6 (3)	74.1
$3s_{1/2}$	24.39 (4)	23.72 (4)	24.35
$3p_{1/2}$	23.13 (8)	23.34 (8)	23.05
$3p_{3/2}$	19.85 (7)	20.16 (8)	19.77
$3d_{3/2}$	11.28 (6)	11.28 (7)	11.21
$3d_{5/2}$	10.53 (6)	10.53 (6)	10.46

Table 7: Recoil correction for a few first states of muonic ^{185}Re . Energy given in eV.

state	$\Delta E_{nk,sphere}^{(rec,rel)}$	$\Delta E_{nk,shell}^{(rec,rel)}$	$\Delta E_{nk,fermi}^{(rec,rel)}$
$1s_{1/2}$	341.7 (5)	328.6 (5)	341.2
$2s_{1/2}$	72.35 (12)	69.89 (11)	72.22
$2p_{1/2}$	85.5 (3)	86.5 (2)	85.2
$2p_{3/2}$	73.5 (2)	74.8 (3)	73.3
$3s_{1/2}$	24.10 (4)	23.43 (4)	24.05
$3p_{1/2}$	22.88 (7)	23.08 (8)	22.80
$3p_{3/2}$	19.64 (7)	19.94 (8)	19.56
$3d_{3/2}$	11.16 (6)	11.17 (7)	11.09
$3d_{5/2}$	10.42 (6)	10.42 (6)	10.36

Table 8: Recoil correction for a few first states of muonic ^{187}Re . Energy given in eV.

state	$\Delta E_{nk,sphere}^{(rec,rel)}$	$\Delta E_{nk,shell}^{(rec,rel)}$	$\Delta E_{nk,fermi}^{(rec,rel)}$
$1s_{1/2}$	413.1 (6)	390.3 (5)	412.6
$2s_{1/2}$	109.23 (16)	103.23 (13)	109.08
$2p_{1/2}$	161.9 (4)	164.2 (4)	161.5
$2p_{3/2}$	142.8 (3)	146.3 (3)	142.4
$3s_{1/2}$	38.87 (6)	37.09(5)	38.82
$3p_{1/2}$	45.82 (10)	46.13 (11)	45.71
$3p_{3/2}$	40.69 (10)	41.50 (11)	40.58
$3d_{3/2}$	26.79 (11)	26.92 (12)	26.67
$3d_{5/2}$	23.79 (10)	23.84 (11)	23.68

Table 9: Recoil correction for a few first states of muonic ^{248}Cm . Energy given in eV.

3.3 Nuclear size sensitivity

We studied the dependence of the recoil correction of the nuclear size. This was done for ^{248}Cm , as well as ^{89}Zr , in order to see the effect on a relatively big and a relatively small atom on the scale of atoms considered in this work. For this we varied the nuclear size by both $\pm 1\%$ and $\pm 0.1\%$. We used the sphere model for this calculation as it seems to fit the results of the Fermi model very well (section 3.4) while being more exact, as less numerical calculation is needed.

One can see in Tables 10 and 11 that the nuclear size, without changing the mass or nuclear charge, indeed has a relevant impact. This mostly holds true for the s states. For ^{248}Cm , the $1s_{1/2}$ state changed around 11 times

the uncertainty for a variation of only 1 percent in size. Thus, this value could very well be used to estimate the nuclear size of heavy atoms. If one, as discussed, assumes the uncertainty smaller than has been done here, this could be used to predict nuclear size to even more precision.

state	$\Delta E_{nk,-1\%}^{(rec,rel)}$	$\Delta E_{nk,-0.1\%}^{(rec,rel)}$	$\Delta E_{nk}^{(rec,rel)}$	$\Delta E_{nk,+0.1\%}^{(rec,rel)}$	$\Delta E_{nk,+1\%}^{(rec,rel)}$
$1s_{1/2}$	136.6	135.7	135.5 (3)	135.4	134.5
$2s_{1/2}$	18.91	18.83	18.82(5)	18.81	18.74
$2p_{1/2}$	9.87	9.89	9.90 (6)	9.90	9.92
$2p_{3/2}$	8.89	8.91	8.92 (6)	8.92	8.94
$3s_{1/2}$	5.578	5.560	5.558 (16)	5.556	5.537
$3p_{1/2}$	2.307	2.315	2.316 (19)	2.316	2.324
$3p_{3/2}$	2.026	2.035	2.036 (18)	2.036	2.045
$3d_{3/2}$	1.432	1.433	1.433 (11)	1.433	1.434
$3d_{5/2}$	1.414	1.415	1.415 (11)	1.415	1.416

Table 10: Recoil effect energy correction for ^{89}Zr by varying nuclear size. Energies given in eV.

state	$\Delta E_{nk,-1\%}^{(rec,rel)}$	$\Delta E_{nk,-0.1\%}^{(rec,rel)}$	$\Delta E_{nk}^{(rec,rel)}$	$\Delta E_{nk,+0.1\%}^{(rec,rel)}$	$\Delta E_{nk,+1\%}^{(rec,rel)}$
$1s_{1/2}$	420.0	413.8	413.1 (6)	412.5	406.4
$2s_{1/2}$	110.39	109.34	109.23 (16)	109.12	108.09
$2p_{1/2}$	163.0	162.0	161.9(4)	161.8	160.8
$2p_{3/2}$	143.4	142.8	142.8 (3)	142.7	142.2
$3s_{1/2}$	39.22	38.91	38.87 (6)	38.84	38.54
$3p_{1/2}$	46.06	45.84	45.82 (10)	45.79	45.58
$3p_{3/2}$	40.80	40.70	40.69 (10)	40.68	40.58
$3d_{3/2}$	26.70	26.78	26.79 (11)	26.80	26.88
$3d_{5/2}$	23.70	23.78	23.79 (10)	23.80	23.87

Table 11: Recoil effect energy correction for ^{248}Cm by varying nuclear size. Energies given in eV.

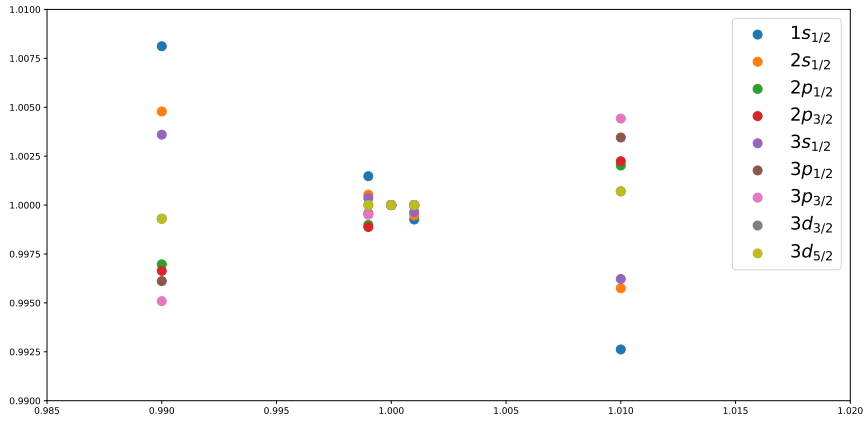


Figure 6: The energy levels for varying nuclear sizes for ^{89}Zr . All values normed to the regular size recoil effect energy correction being 1.

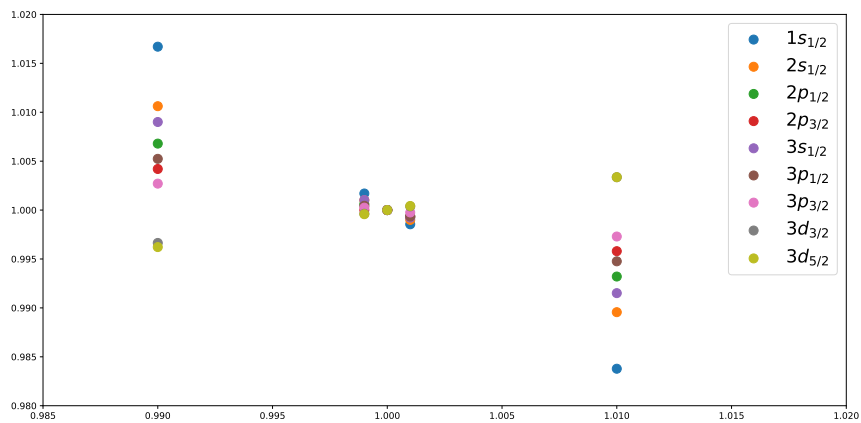


Figure 7: The energy levels for varying nuclear sizes for ^{248}Cm . All values normed to the regular size recoil effect energy correction being 1.

3.4 Numerical accuracy

Here we calculated the s states of ^{248}Cm for different numbers of splines, for both the Fermi and sphere model. This should give an idea of the numerical error of the calculation. We also present the value of the numerical calculation for the sphere model, to show how similar it behaves to the Fermi model.

As one can see in Tables 12, 13 and 14 below, the semi-analytical values only changed in the eighth digit and changed less the higher the spline-numbers were. They thus seemed to be quite heavily converging to a value that was at most different in the tenth digit from the 90 splines value. It is also interesting to see that while for each state the value either monotonically increases or decreases with the number of splines, it depended on the state whether it in or decreased.

The numerical calculation already changed in the fourth digit. They seemed to converge towards the semi-analytical values, while always being smaller. This was the case for all isotopes considered in this work.

Interestingly, the Fermi model results differed only slightly from the numerical sphere model results, while always being slightly bigger for the s states. This makes sense as the models are very similar and with the Fermi distribution being slightly denser in the center of the core. Therefore, as seen in section 3.3, the s states are expected to be slightly increased, while some other states might slightly decrease.

It leads to the conclusion that even if one looks for nuclear recoil effect values for the Fermi model, the best values for this will be the semi-analytical sphere model calculations. The real values for the Fermi model will be slightly bigger yet most likely well within the given uncertainty, and all but certainly these values match the reality better than the numerical Fermi calculations.

Number of splines	$\Delta E_{nk,sphere}^{(rec,rel)}$	$\Delta E_{nk,sphere,num}^{(rec,rel)}$	$\Delta E_{nk,fermi}^{(rec,rel)}$
30	413.1364757	411.81	411.91
50	413.1364387	412.35	412.40
70	413.1364376	412.57	412.61
90	413.1364373	412.70	412.72

Table 12: Recoil correction to the ^{248}Cm $1s$ state for different numbers of splines. Energies given in eV.

Number of splines	$\Delta E_{nk,sphere}^{(rec,rel)}$	$\Delta E_{nk,sphere,num}^{(rec,rel)}$	$\Delta E_{nk,fermi}^{(rec,rel)}$
30	109.23089713	108.870	108.878
50	109.23089950	109.013	109.016
70	109.23089967	109.075	109.077
90	109.23089968	109.109	109.110

Table 13: Recoil correction to the ^{248}Cm $2s$ state for different numbers of splines. Energies given in eV.

Number of splines	$\Delta E_{nk,sphere}^{(rec,rel)}$	$\Delta E_{nk,sphere,num}^{(rec,rel)}$	$\Delta E_{nk,fermi}^{(rec,rel)}$
30	38.874882328	38.738	38.740
50	38.874883186	38.792	38.793
70	38.874883247	38.816	38.816
90	38.874883257	38.829	38.829

Table 14: Recoil correction to the ^{248}Cm $3s$ state for different numbers of splines. Energies given in eV.

3.5 Different uncertainties in comparison

There are different uncertainties playing a role in the calculation of the nuclear recoil effect energy correction.

As discussed above, when only considering the sphere and Fermi nuclear model, the uncertainty by nuclear model can be disregarded on the considered scale. This should also be a viable assumption for all realistic nuclear models, as it is unlikely that they heavily deviate from either of those two models.

There is also the uncertainty of the used method. It is hard to make an assumption on this uncertainty. While another model of calculation could be used for comparison, yet there is none at our disposal right now. Thus, we will ignore this uncertainty for the moment.

Two assumptions can be made for the uncertainty of the numerical calculations. First, as done throughout this work, one can calculate the difference of the results of the semi-analytical and the numerical approach towards calculating the sphere model nuclear recoil energy correction. The merit to this is that, while the semi-analytical approach is all but certainly more accurate, it also contains some numerical calculation. Therefore, one could assume the uncertainty to be of similar size as the difference of the two calculations.

One might also assume that as the energy correction values of the semi-analytical approach seem to converge with increasing number of splines, as can be seen in subsection 3.4, this can be used to approximate the calcula-

tional accuracy. In this case the uncertainty would be yet way smaller than the uncertainty of the model and could be considered as zero.

Finally, there is the uncertainty by nuclear parameters. As the considered models discard any angular dependence, here one can only consider nuclear size and weight. Here, the uncertainty of the nuclear RMS radius, given by [7], is far more significant than the uncertainty of the weight.

Tables 15 and 16 contain the nuclear recoil energy correction for all considered isotopes as well as states for the sphere nuclear model, with both the uncertainty by calculating the difference between the semi-analytical and numerical energy correction in the first brackets, and the uncertainty by nuclear size, assumed by Eq.(23), with $\Delta_{tot}R$ being the uncertainty given in [7]:

$$\Delta E_{nk,size}^{(rec,rel)}(rm_{nucl}) = E_{nk}^{(rec,rel)}(rm_{nucl} - \Delta_{tot}R) - E_{nk}^{(rec,rel)}(rm_{nucl} + \Delta_{tot}R) \quad (23)$$

One can see, that depending on the isotope's size uncertainty, either the uncertainty by numerical calculation dominates, or for the first few states the uncertainty by nuclear size dominates.

state	^{89}Zr	^{119}Sn	^{147}Sm	^{185}Rm
$1s_{1/2}$	135.5 (3)(0.5)	207.8 (4)(2)	288.4 (5)(5)	346.4 (5)(32)
$2s_{1/2}$	18.82(5)(0.4)	32.78 (8)(2)	52.48 (10)(6)	73.26 (12)(43)
$2p_{1/2}$	9.90 (6)(0.1)	22.82 (12)(0.4)	48.72 (19)(0.07)	86.5 (3)(14)
$2p_{3/2}$	8.92 (6)(0.1)	19.93 (11)(0.5)	41.78 (19)(1.2)	74.3 (2)(0.06)
$3s_{1/2}$	5.558 (16)(1)	10.03 (2)(0.5)	16.72 (3)(1.5)	24.39 (4)(12)
$3p_{1/2}$	2.316 (19)(0.4)	5.63 (3)(0.1)	12.57 (5)(0.2)	23.13 (8)(2)
$3p_{3/2}$	2.036 (18)(0.4)	4.81 (3)(0.2)	10.64 (5)(0.5)	19.85 (7)(1.4)
$3d_{3/2}$	1.433 (11)(0.04)	2.98 (2)(0.03)	6.07 (4)(0.2)	11.28 (6)(2)
$3d_{5/2}$	1.415 (11)(0.03)	2.92 (2)(0.02)	5.82 (4)(0.13)	10.53 (6)(1.7)

Table 15: Nuclear recoil effect energy correction for ^{89}Zr , ^{119}Sn , ^{147}Sm , ^{185}Rm and ^{187}Rm . Uncertainty by numerical calculation in the first brackets, uncertainty by nuclear parameters in the second brackets. Uncertainties given in units of last given digit. Energies given in eV.

state	^{187}Rm	^{208}Pb	^{205}Bi	^{248}Cm
$1s_{1/2}$	372.0 (5)(3)	389.1 (6)(11)	413.1 (6)(45)	341.7 (5)(32)
$2s_{1/2}$	84.64 (13)(4)	89.27 (14)(14)	109.23 (16)(76)	72.35 (12)(43)
$2p_{1/2}$	109.5 (3)(0.2)	116.5 (3)(0.8)	161.9 (4)(7)	85.5 (3)(14)
$2p_{3/2}$	94.6 (3)(0.06)	100.7 (3)(0.2)	142.8 (3)(4)	73.5 (2)(0.06)
$3s_{1/2}$	28.80 (5)(0.9)	30.45 (5)(4)	38.87 (6)(22)	24.10 (4)(12)
$3p_{1/2}$	29.80 (9)(0.4)	31.79 (9)(1.7)	45.82 (10)(16)	22.88 (7)(2)
$3p_{3/2}$	25.80 (8)(0.018)	27.54 (9)(0.13)	40.69 (10)(7)	19.64 (7)(1.3)
$3d_{3/2}$	15.11 (8)(0.2)	16.20 (8)(0.8)	26.79 (11)(6)	11.16 (6)(2)
$3d_{5/2}$	13.87 (7)(0.2)	14.84 (8)(0.7)	23.79 (10)(5)	10.42 (6)(1.7)

Table 16: Nuclear recoil effect energy correction for ^{208}Pb , ^{205}Bi and ^{248}Cm . Uncertainty by numerical calculation in the first brackets, uncertainty by nuclear parameters in the second brackets. Uncertainties given in units of last given digit. Energies given in eV.

3.6 Different models

Classically, nuclear recoil corrections are calculated by using the reduced mass, $\mu = \frac{mM}{m+M}$ and expanding to low orders of αZ . For high Z atoms $\alpha Z \approx 1$, so this approach is not viable anymore. In [10] this is solved for $Z \approx 10 - 40$ by expanding up to $(\alpha Z)^4$. This approach should also give approximate values for higher Z . That leads to:

$$\Delta E_{M,rel} = \left(-\frac{29}{48} + \ln \frac{9}{8} \right) (\alpha Z)^2 \Delta E_{M,nr}^{(0)}, \quad (24)$$

with $\Delta E_{M,nr}^{(0)}$ being the non-relativistic nuclear recoil contributions of the zeroth order in $1/Z$ given by:

$$\Delta E_{M,nr}^{(0)} = -\frac{2^9 (\alpha Z)^2 m^2}{3^8 M}. \quad (25)$$

In [2, 3], instead of expanding in terms of αZ , it was expanded in terms of $\frac{m}{M}$, using the quasipotential approach. The calculation was carried out numerically. The results for low Z atoms were compared to earlier results of calculations expanding in αZ and found good agreement. This formalism should in theory allow to calculate the nuclear recoil correction for high Z atoms. The transition energies for high Z lithium-like atoms were calculated as well. It was found that the recoil correction for the $(1s)^2 2p_{1/2} (1s)^2 2s_{1/2}$ transition of lithium-like uranium is comparable to the experimental uncertainty and thus should be important for the comparison of experiment and theory.

4 Model dependence and outlook

In this work, the nuclear recoil effect energy correction for muonic atoms was calculated to higher accuracy than before. This is useful to crosscheck it with experimental data, as in [11], in order to learn more about the nuclear structure.

We investigated model dependence, numerical convergence and nuclear parameter dependence, and found that, if only considering the sphere and Fermi nuclear models, the uncertainty originating from nuclear parameters is the dominant one for some isotopes, while the uncertainty originating from the calculation dominates for others. The uncertainty of the method is not considered in this part as it is not possible to make an assumption on it, yet it should not be forgotten that it might play a relevant role in the consideration. If one makes a different assumption for the calculational uncertainty, the nuclear size uncertainty dominates all other uncertainties for all states and isotopes.

The energy correction was calculated for different nuclear models, the shell model, the sphere model and the Fermi model. It was found that the sphere and Fermi model energy corrections are very similar and that using the sphere model in the context of this work is better, as it is calculated by the more precise method.

In future, one could formulate a semi-analytical way of calculating the energy correction for the Fermi model, as this would lead to more accuracy in the calculation.

Acknowledgements

I want to thank Natalia Oreshkina for all the time she spend helping me with this work, I could not have done it without her help. I would also like to thank Margot Chazotte and Linus von Klitzing, for proofreading this work. Lastly I want to thank the MPIK staff, especially the IT staff for setting me up with the MPIK cluster and being helpful for clearing up technical issues.

References

- [1] Niklas Michel. “Relativistic theory of nuclear structure effects in heavy atomic systems”. PhD thesis. Jan. 2019.
- [2] A. N. Artemyev, V. M. Shabaev, and V. A. Yerokhin. “Relativistic nuclear recoil corrections to the energy levels of hydrogenlike and high- Z lithiumlike atoms in all orders in αZ ”. In: *Phys. Rev. A* 52 (3 1995), pp. 1884–1894. DOI: [10.1103/PhysRevA.52.1884](https://doi.org/10.1103/PhysRevA.52.1884). URL: <https://link.aps.org/doi/10.1103/PhysRevA.52.1884>.
- [3] A. N. Artemyev, V. M. Shabaev, and V. A. Yerokhin. “Nuclear recoil corrections to the $2p_{3/2}$ state energy of hydrogen-like and high- Z lithium-like atoms in all orders in αZ ”. In: *Journal of Physics B: Atomic, Molecular and Optical Physics* 28.24 (1995), pp. 5201–5206. DOI: [10.1088/0953-4075/28/24/006](https://doi.org/10.1088/0953-4075/28/24/006). URL: <https://doi.org/10.1088/0953-4075/28/24/006>.
- [4] E. Borie and G. A. Rinker. “The energy levels of muonic atoms”. In: *Rev. Mod. Phys.* 54 (1 1982), pp. 67–118. DOI: [10.1103/RevModPhys.54.67](https://doi.org/10.1103/RevModPhys.54.67). URL: <https://link.aps.org/doi/10.1103/RevModPhys.54.67>.
- [5] W. R. Johnson, S. A. Blundell, and J. Sapirstein. “Finite basis sets for the Dirac equation constructed from B splines”. In: *Phys. Rev. A* 37 (2 1988), pp. 307–315. DOI: [10.1103/PhysRevA.37.307](https://doi.org/10.1103/PhysRevA.37.307). URL: <https://link.aps.org/doi/10.1103/PhysRevA.37.307>.
- [6] V. M. Shabaev et al. “Dual Kinetic Balance Approach to Basis-Set Expansions for the Dirac Equation”. In: *Phys. Rev. Lett.* 93 (13 2004), p. 130405. DOI: [10.1103/PhysRevLett.93.130405](https://doi.org/10.1103/PhysRevLett.93.130405). URL: <https://link.aps.org/doi/10.1103/PhysRevLett.93.130405>.
- [7] I. Angeli and K. P. Marinova. “Table of experimental nuclear ground state charge radii: An update”. In: *Atomic Data and Nuclear Data Tables* 99.1 (Jan. 2013), pp. 69–95. DOI: [10.1016/j.adt.2011.12.006](https://doi.org/10.1016/j.adt.2011.12.006).
- [8] <https://www.ndc.jaea.go.jp/NuC/index.html>.
- [9] F. A. Parpia and A. K. Mohanty. “Relativistic basis-set calculations for atoms with Fermi nuclei”. In: *Phys. Rev. A* 46 (7 1992), pp. 3735–3745. DOI: [10.1103/PhysRevA.46.3735](https://doi.org/10.1103/PhysRevA.46.3735). URL: <https://link.aps.org/doi/10.1103/PhysRevA.46.3735>.

- [10] V.M. Shabaev and A.N. Artemyev. “Relativistic nuclear recoil corrections to the energy levels of multicharged ions.” In: *Journal of Physics B: Atomic, Molecular and Optical Physics* 27.7 (1994), pp. 1307–1314. DOI: [10.1088/0953-4075/28/24/006](https://doi.org/10.1088/0953-4075/28/24/006). URL: <https://doi.org/10.1088/0953-4075/28/24/006>.
- [11] A. Antognini et al. “Measurement of the quadrupole moment of ^{185}Re and ^{187}Re from the hyperfine structure of muonic X rays”. In: *Physical Review C* 101.5 (2020). ISSN: 2469-9993. DOI: [10.1103/physrevc.101.054313](https://doi.org/10.1103/physrevc.101.054313). URL: <http://dx.doi.org/10.1103/PhysRevC.101.054313>.

Erklärung

Ich versichere, dass ich diese Arbeit selbstständig verfasst und keine anderen als die angegebenen Quellen und Hilfsmittel benutzt habe.

Heidelberg, den 8.7.2022

R. Charlotte